# Secondary calcification and dissolution respond differently to future ocean conditions.

**N. J. Silbiger[1] and M. J. Donahue[1]**

[1] {University of Hawai‘i at Mānoa, Hawai‘i Institute of Marine Biology, PO Box 1346, Kāne‘ohe, Hawai‘i, 96744}

Correspondence to: N.J. Silbiger (silbiger@hawaii.edu)

## Abstract

Climate change threatens both the accretion and erosion processes that sustain coral reefs. Secondary calcification, bioerosion, and reef dissolution are integral to the structural complexity and long-term persistence of coral reefs, yet these processes have received less research attention than reef accretion by corals. In this study, we use climate scenarios from RCP 8.5 to examine the combined effects of rising ocean acidity and SST on both secondary calcification and dissolution rates of a natural coral rubble community using a flow-through aquarium system. We found that secondary reef calcification and dissolution responded differently to the combined effect of $pCO_2$ and temperature. Calcification had a non-linear response to the combined effect of $pCO_2$- temperature: the highest calcification rate occurred slightly above ambient conditions and the lowest calcification rate was in the highest $pCO_2$-temperature condition. In contrast, dissolution increased linearly with $pCO_2$-temperature. The rubble community switched from net calcification to net dissolution at +271 µatm $pCO_2$ and 0.75° C above ambient conditions, suggesting that rubble reefs may shift from net calcification to net dissolution before the

end of the century. Our results indicate that (i) dissolution may be more sensitive to climate change than calcification and (ii) that calcification and dissolution have different functional responses to climate stressors; this highlights the need to study the effects of climate stressors on both calcification and dissolution to predict future changes in coral reefs.

## 1 Introduction

In 2013, atmospheric carbon dioxide ($CO_{2(atm)}$) reached an unprecedented milestone of 400 ppm (Tans and Keeling, 2013), and this rising $CO_{2(atm)}$ is increasing sea-surface temperature (SST) and ocean acidity (Caldeira and Wickett, 2003;Cubasch et al., 2013;Feely et al., 2004). Global SST has increased by 0.78°C since pre-industrial times (Cubasch et al., 2013), and it is predicted to increase by another 0.8-5.7°C by the end of this century (Meinshausen et al., 2011;Van Vuuren et al., 2008;Rogelj et al., 2012). The Hawai`i Ocean Time-series detected a 0.075 decrease in mean annual pH at Station ALOHA over the past 20 years (Doney et al., 2009) and there have been similar trends at stations around the world including the Bermuda Atlantic Time-series and the European Station for Time-series Observations in the ocean (Solomon et al. 2007). pH is expected to drop by an additional 0.14-0.35 pH units by the end of the 21$^{st}$ century (Bopp et al., 2013). All marine ecosystems are at risk from rising SST and decreasing pH (Doney et al., 2009;Hoegh-Guldberg et al., 2007;Hoegh-Guldberg and Bruno, 2010), but coral reefs are particularly vulnerable to these stressors (reviewed in Hoegh-Guldberg et al., 2007).

Corals create the structurally complex calcium carbonate ($CaCO_3$) foundation of coral reef ecosystems. This structural complexity is at risk from climate-driven shifts from high-complexity, branched coral species to mounding and encrusting growth forms (Fabricius et al., 2011) and from increases in the natural processes of reef destruction, including bioerosion and dissolution (Wisshak et al., 2012, 2013;Tribollet et al., 2006). While substantial research attention has focused on the response of reef-building corals to climate change (reviewed in Hoegh-Guldberg et al., 2007;Fabricius, 2005;Pandolfi et al., 2011), secondary calcification (calcification by non-coral invertebrates and calcareous algae), bioerosion, and reef dissolution that are integral to maintaining the structural complexity and net growth of coral reefs has received less attention (Andersson and Gledhill, 2013;Andersson et al., 2011;Andersson and Mackenzie, 2012). Bioerosion and dissolution breakdown the reef framework while secondary calcification helps maintain reef stability by cementing the reef together (Adey, 1998; Camoin and Montaggioni, 1994; Littler, 1973) and producing chemical cues that induce settlement of many invertebrate larvae including several species of corals (Harrington et al. 2004; Price 2010). Coral reefs will only persist if constructive reef processes (growth by corals and secondary calcifiers) exceed destructive reef processes (bioerosion and dissolution). In this study, we examine the combined effects of rising ocean acidity and SST on both calcification and dissolution rates of a natural community of secondary calcifiers and bioeroders.

Recent laboratory experiments have focused on the response of individual taxa of bioeroders or secondary calcifiers to climate stressors. For example, studies have specifically addressed the effects of rising ocean acidity and/or temperature on bioerosion

69 by a *Clionid* sponge (Wisshak et al., 2012, 2013;Fang et al., 2013) and a community of
70 photosynthesizing microborers (Tribollet et al., 2009;Reyes-Nivia et al., 2013). These
71 studies found that bioerosion increased under future climate change scenarios. Several
72 studies have focused on tropical calcifying algae and have found decreased calcification
73 (Semesi et al., 2009; Johnson et al., 2014; Comeau et al., 2013;Jokiel et al., 2008;Kleypas
74 and Langdon, 2006) and increased dissolution (Diaz-Pulido et al., 2012) with increasing
75 ocean acidity and/or SST. However, the bioeroding community is extremely diverse and
76 can interact with the surrounding community of secondary calcifiers: for example,
77 crustose coralline algae (CCA) can inhibit internal bioerosion (White, 1980;Tribollet and
78 Payri, 2001). To understand the combined response of bioeroders and secondary
79 calcifiers, we take a community perspective and examine the synergistic effects of rising
80 SST and ocean acidity on a natural community of secondary calcifiers and bioeroders.
81 Using the total alkalinity anomaly technique, we test for net changes in calcification
82 during the day and dissolution (most of which is caused by bioeroders; Andersson and
83 Gledhill, 2013) at night. Our climate change treatments are modelled after the
84 Representative Concentration Pathway (RCP) 8.5 climate scenario (Van Vuuren et al.,
85 2011;Meinshausen et al., 2011), one of the high emissions scenarios used in the most
86 recent Intergovernmental Panel on Climate Change (IPCC) report (Cubasch et al., 2013).
87 The RCP 8.5 scenario predicts an increase in temperature of 3.8 – 5.7°C (Rogelj et al.,
88 2012) and an increase in atmospheric $CO_2$ of 557 ppm by the year 2100 (Meinshausen et
89 al., 2011). We use the RCP 8.5 scenario because the current $CO_2$ concentrations are
90 tracking just above what this scenario predicts (Sanford et al., 2014). While prior studies
91 have focused on the contributions of individual community members to increased

temperature and $CO_2$; here, we examine the community response to the RCP 8.5 climate scenario and measure calcification, dissolution, and net community production rates.

## 2 Materials and Methods

### 2.1 Collection Site

All collections were made on the windward side of Moku o Loʻe (Coconut Island) in Kāneʻohe Bay, Hawaiʻi adjacent to the Hawaiʻi Institute of Marine Biology. This fringing reef is dominated by *Porites compressa* and *Montipora capitata*, with occasional colonies of *Pocillopora damicornis*, *Fungia scutaria*, and *Porites lobata*. Kāneʻohe Bay is a protected, semi-enclosed embayment; the residence time can be >1 month long in the protected southern portion of the Bay (Lowe et al., 2009a;Lowe et al., 2009b) that is coupled with a high daily variance in pH (Guadayol et al., 2014). The wave action is minimal (Smith et al., 1981;Lowe et al., 2009a;Lowe et al., 2009b) and currents are relatively slow (5cm $s^{-1}$ maximum) and wind-driven (Lowe et al., 2009a;Lowe et al., 2009b).

### 2.2 Sample Collection

We collected pieces of dead *Porites compressa* coral skeleton (hereafter, referred to as rubble) as representative communities of bioeroders and secondary calcifiers. Rubble was collected with a hammer and chisel from a shallow reef flat (~1m depth) in November, 2012. Only pieces of rubble without any live coral were collected. The rubble community in Kāneʻohe Bay is comprised of secondary calcifiers, including CCA from the genera *Hydrolithon, Sporolithon,* and *Peyssonnelia* and non-coral calcifying invertebrates (e.g. boring bivalves (*Lithophaga fasciola* and *Barbatia divaricate*), oysters (*Crassostrea*

*gigas*), and small crustaceans); filamentous and turf algae; and internal bioeroders, including boring bivalves (*L. fasciola* and *B.divaricate*), sipunculids (*Aspidosiphon elegans*, *Lithacrosiphon cristatus*, *Phascolosoma perlucens*, and *Phascolosoma stephensoni*), phoronids (*Phoronis ovalis*), sponges (*Cliona* spp.) and a diverse assemblage of polychaetes (White, 1980). All rubble pieces were combined after collection and maintained in a 100L flow-through tank with ambient seawater from Kāneʻohe Bay until random assignment to treatments.

## 2.3. Experimental Design

The Hawaiʻi Institute of Marine Biology (HIMB) hosts a mesocosm facility with flow-through seawater from Kāneʻohe Bay and controls for light, temperature, $pCO_2$, and flow rate. The facility is comprised of 24 experimental aquaria split between four racks; each rack has a 150L header tank which feeds 6 experimental aquaria, each 50L in volume (Figure 1).

Before adding rubble to the experimental aquaria, we collected day and night samples of pH, total alkalinity (TA), temperature, and salinity from all aquaria to demonstrate the consistency of water conditions across aquaria without any rubble present (Table 1). The long-term temporal stability of the mesocosm system is reported in Putnam (2012). We then conducted "control" and "treatment" experiments to determine how RCP 8.5 predictions affect daytime calcification and nighttime dissolution rates in a natural rubble community. The first "control experiment" characterized baseline calcification and dissolution in each aquarium caused by differences in rubble communities. In the second "treatment experiment", we manipulated $pCO_2$ and

136 temperature to simulate four climate scenarios (pre-industrial, present day, 2050, and
137 2100) and tested the response of calcification, dissolution, and net community
138 production. Each experiment used the TA anomaly method (Smith and Key, 1975;
139 Andersson et al., 2009). This method calculates net calcification from changes in total
140 alkalinity, and calculates net community production from changes in total dissolved
141 inorganic carbon adjusted for changes in carbon due to calcificaiton. Because estimates
142 of calcification are based on changes in total alkalinity, this method does not account for
143 mechanical erosion (e.g., small chips of $CaCO_3$ produced by sponge erosion). However,
144 given the short duration of the experiment and the types of bioeroders present, we expect
145 that chemical dissolution captured a significant proportion of the erosion in the system.
146 Approximately 1.2L of rubble (3-4 pieces of weight 499 ± 148 g and skeletal
147 density 1.53 ± 0.1 g $cm^{-3}$ (mean ± SD, n=85)) were placed in each of the 24 experimental
148 aquaria and acclimated to tank conditions in ambient seawater for three days. On the
149 fourth day, we performed the control experiment, calculating daytime calcification and
150 nighttime dissolution for rubble in ambient seawater conditions using the TA anomaly
151 technique. The next day we manipulated seawater $pCO_2$ and temperature to replicate four
152 climate scenarios for the treatment experiment: pre-industrial (-1±0.057°C and -205±11.9
153 µatm), present day (natural Kāneʻohe Bay seawater 24.8±0.09 °C, 614±15.6 µatm), 2050
154 (+1.4±0.09 °C and +255±31 µatm), and 2100 (+2.4±0.08 and +433±40 µatm). Note that
155 all changes in temperature and $pCO_2$ were made relative to present day Kāneʻohe Bay
156 seawater conditions: $pCO_2$ in Kāneʻohe Bay is consistently high relative to the open
157 ocean and can range from 196-976 µatm in southern Kāneʻohe bay depending on
158 conditions (Drupp et al., 2013). The yearly average $pCO_2$ at our collection site ranged

159 from 565-675 µatm (Silbiger et al., 2014). After an acclimation time of seven days, we
160 sampled the treatment experiment, calculating daytime calcification and nighttime
161 dissolution over a 24 hour period.

162 During both experiments, TA, pH, salinity, temperature, and dissolved inorganic
163 nutrient (DIN) samples were collected every 12 hours over a 24 hour period: just before
164 lights-on in the morning (time 1) and just before lights-off at night (time 2) to capture
165 light conditions, and then again before lights-on the next morning (time 3) to capture dark
166 conditions. Flow into each aquarium was monitored and adjusted every three hours to
167 ensure a consistent flow rate over the 24 hour experiment. We calculated net ecosystem
168 calcification, dissolution, and net community production using a simple box model
169 (Andersson et al., 2009) and normalized all our calculations to the surface area of the
170 rubble in each tank. Surface area of the rubble was calculated using the wax dipping
171 technique (Stimson and Kinzie III, 1991) at the end of the experiment.

172 **2.4 Mesocosm Set-up**

173 The mesocosm facility (Figure 1) is supplied with ambient seawater from
174 Kāneʻohe Bay, which is filtered through a sand filter, passed through a water chiller
175 (Aqualogic Multi Temp MT-1 Model # 2TTB3024A1000AA), and then fed into one of
176 the four header tanks. $pCO_2$ was manipulated using a $CO_2$ gas blending system (see
177 Fangue et al., 2010; Johnson and Carpenter, 2012). Each target $pCO_2$ concentration was
178 created by mixing $CO_2$-free atmospheric air with pure $CO_2$ using mass flow controllers
179 (C100L Sierra Instruments). Output $pCO_2$ was analyzed using a calibrated infrared
180 $CO_2$ analyzer (A151, Qubit Systems). $CO_2$ mixtures were then bubbled into one of the

four header tanks and water from each individual header tank fed into the six individual treatment aquaria (Figure 1). The $pCO_2$ in each treatment aquarium was estimated with CO2SYS (Van Heuven et al., 2009) using pH and TA as the parameters.

Temperature was manipulated in each treatment aquarium using dual-stage temperature controllers (Aqualogic TR115DN). The temperature was continuously monitored with temperature loggers (TidbiT v2 Water Temperature Data Logger, sampling every 20 min) and point measurements were taken during every sampling period with a handheld digital thermometer (Traceable Digital Thermometer, Thermo Fisher Scientific; precision = 0.001 °C). Light was controlled by positioning an oscillating pendant metal-halide light (250 W) over a set of three aquaria and was programmed to emit an equal amount of light to each tank (~500µE of light). Lights were set to a 12:12 hour photoperiod and were monitored using a LI-COR spherical quantum PAR sensor. Flow rate was maintained at 115±1 ml $min^{-1}$, resulting in a residence time of 7.3±0.07 hours per tank. Each aquarium was equipped with a submersible powerhead pump (Sedra KSP-7000 powerhead) to ensure that the tank was well-mixed.

### 2.5 Seawater Chemistry

All sample collection and storage vials were cleaned in a 10% HCl bath for 24 hours and rinsed three times with MilliQ water before use and rinsed three times with sample water during sample collection and processing.

#### 2.5.1 Total Alkalinity

Duplicate TA samples were collected in 300 ml borosilicate sample containers with glass stoppers. Each sample was preserved with 100µL of 50% saturated $HgCl_2$ and analyzed

within 3 days using open cell potentiometric titrations on a Mettler T50 autotitrator (Dickson et al., 2007). A Certified Reference Material (CRM - Reference Material for Oceanic $CO_2$ Measurements, A. Dickson, Scripps Institution of Oceanography) was run at the beginning of each sample set. The accuracy of the titrator never deviated more than ±0.8% from the standard, and TA measurements were corrected for these deviations. The precision was 3.55µEq (measured as standard deviation of the duplicate water samples). During the 24-hour control experiment the average changes in TA were 37µEq over the day and 20µEq over the night (day and night TA changes were of larger magnitude in the treatment experiments): these are measurable changes given the precision and accuracy of the TA measurements.

### 2.5.2 $pH_t$ (total scale)

Duplicate $pH_t$ samples were collected in 20ml borosilicate glass vials, brought to a constant temperature of 25ºC in a water bath, and immediately analyzed using an m-cresol dye addition spectrophotometric technique (Dickson et al., 2007). Accuracy of the pH was tested against a Tris buffer of known $pH_t$ from the Dickson Lab at Scripps Institution of Oceanography (Dickson et al., 2007). Our accuracy was better than ±0.04%, and the precision was 0.004 pH units (measured as standard deviation of the duplicate water samples). *In situ* pH and the remaining carbonate parameters were calculated using CO2SYS (Van Heuven et al., 2009) with the following measured parameters: $pH_t$, TA, temperature, and salinity. The K1K2 apparent equilibrium constants were from Mehrbach (1973) and refit by Dickson & Millero (1987) and $HSO_4^-$ dissociation constants were taken from Uppström (1974) and Dickson (1990).

### 2.5.3 Salinity

Duplicate salinity samples were analyzed on a Portasal 8410 portable salinometer calibrated with an OSIL IAPSO standard (accuracy = ±0.003 psu, precision = ±0.0003 psu).

### 2.5.4 Nutrients

Nutrient samples were collected with 60ml plastic syringes and immediately filtered through combusted 25mm glass fiber filters (GF/F 0.7µm) and transferred into 50ml plastic centrifuge tubes. Nutrient samples were frozen and later analyzed for $Si(OH)_4$, $NO_3^-$, $NO_2^-$, $NH_4^+$, and $PO_4^{3-}$ on a Seal Analytical AA3 HR Nutrient Analyzer at the UH SOEST Lab for Analytical Chemistry.

## 2.6 Measuring Net Ecosystem Calcification

We assumed that the mesocosms were well mixed systems; thus, we calculated net ecosystem calcification and net communtity photosynthesis following the simple box model presented in Andersson et al. (2009). TA was normalized to a constant salinity (35 psu) to account for changes due to evaporation and then corrected for dissolved inorganic nitrogen and phosphate to account for their small contributions to the acid-base system (Wolf-Gladrow et al., 2007). Net ecosystem calcification, or G, was calculated using the following equation:

$$G = \left[F_{TAin} - F_{TAout} - \frac{d\mathrm{TA}}{dt}\right]/2 \qquad \text{Eq. 1}$$

where $F_{TAin}$ is the rate of TA flowing into an aquarium ( = average TA in the header tank times the inflow rate), $F_{TAout}$ is the rate of TA flowing out of an aquarium ( = average

TA in the aquarium times the outflow rate), and , $\frac{\mathrm{dTA}}{\mathrm{dt}}$ is the change in TA in an aquarium during the measurement period (change in TA normalized to the volume of water and the surface area of the rubble); specific calculations are given in the supplemental material. The equation is divided by two because one mole of $CaCO_3$ is precipitated or dissolved for every two moles of TA removed or added to the water column. Here, G represents the sum of all the calcification processes minus the sum of all the dissolution processes in mmol $CaCO_3$ $m^{-2}$ $hr^{-1}$; thus, all positive numbers are net calcification, and all negative numbers are negative net calcification (i.e., net dissolution). Net daytime calcification ($G_{day}$) is calculated from the first 12 hour sampling period in the light, net nighttime dissolution ($G_{night}$) is calculated from the second 12 hour sampling period in the dark, and total net calcification ($G_{net}$) is calculated from the full 24 hour cycle ($G_{day}$ + $G_{night}$). $G_{day}$, $G_{night}$, and $G_{net}$ are converted from hourly to daily rates and presented as mmol $CaCO_3$ $m^{-2}$ $d^{-1}$.

## 2.7 Measuring Net Community Production and Respiration

Net community production (NCP) was calculated by measuring changes in DIC (Gattuso et al., 1999). DIC was normalized to a constant salinity (35 psu) to account for any evaporation over the 24 hour period. We used a simple box model to calculate NCP:

$$NCP = \left[F_{\mathrm{DIC}in} - F_{\mathrm{DIC}out} - \frac{d\mathrm{DIC}}{dt}\right] - G \qquad \text{Eq. 2}$$

$F_{\mathrm{DIC}in}$, $F_{\mathrm{DIC}out}$, and $\frac{d\mathrm{DIC}}{dt}$ are the rates of DIC flowing into the aquaria, flowing out of the aquaria, and the change in DIC in the aquaria per unit time in mmol C $m^{-2}$ $hr^{-1}$, respectively. To measure NCP, we subtract G to remove any change in carbon due to

inorganic processes. NCP represents the sum of all the photynthetic processes minus the sum of all the respiration processes, thus all positive numbers are net photosynthesis and all negative numbers are negative net photosynthesis (i.e., net respiration). Net daytime NCP ($NCP_{day}$) is calculated from the first 12 hour sampling period in the light, net nightime NCP ($NCP_{night}$) is calculated from the second 12 hour sampling period in the dark, and total NCP ($NCP_{net}$) is calculated from the full 24 hour cycle ($NCP_{day}$ + $NCP_{night}$). All rates are presented as mmol C $m^{-2}$ $d^{-1}$.

## 2.8 Statistical Analysis

Each aquarium contained a slightly different rubble community because of the randomization of rubble pieces to each treatment. To ensure there were no systematic differences in rubble communities between racks (rack effects) before the experimental treatments were applied, we tested for differences in calcification and NCP between racks in the control experiment using an ANOVA (Figure A2).

In the treatment experiment, we first tested for feedbacks in carbonate chemistry due to the presence of rubble: using a paired t-test, we compared the day-night difference in measured $pCO_2$ in each aquarium with rubble, $\left(pCO_{2,day} - pCO_{2,night}\right)_{rubble}$, and without rubble, $\left(pCO_{2,day} - pCO_{2,night}\right)_{no\ rubble}$.

Although we imposed four discrete temperature-$pCO_2$ scenario treatments on each tank (Table 1), random variation between treatments and the feedback between the rubble communities and the water chemistry resulted in near-continuous variation in temperature-$pCO_2$ treatments across aquaria (Figures 2 and A1). To capture this

continuous variation in temperature-$pCO_2$ in the analysis, we used the measured temperature-$pCO_2$ seawater condition as a continuous independent variable in a regression rather than the four categorical treatment conditions in an ANOVA (an analysis of G and NCP using the ANOVA approach is included in Figures A3, A4 and Tables A1, A2). The regression approach allowed us to better capture the quantitative relationships between net calcification (G) or NCP and the temperature-$pCO_2$ treatment. We created a single, continuous variable, Standardized Climate Change (SCC), from a linear combination of temperature and $pCO_2$ values in each aquarium. A simple linear combination was used because $pCO_2$ increased linearly with temperature (Figure 2), as imposed by our treatments. We first calculated the relationship between ΔTemp (Eq 3) and $\Delta pCO_2$ (Eq 4) using linear regression. The coefficients from this regression (slope: $\alpha$ = 0.0031; y-intercept: $\beta$ = - 0.078) were used to combine $pCO_2$ and temperature onto the same scale, as a measure of Standardized Climate Change (Eq 5):

$$\Delta Temp_i = Temp_{trt,i} - Temp_{cont,i} \quad \text{Eq. 3}$$

$$\Delta pCO_{2_i} = pCO_{2_{trt,i}} - pCO_{2_{cont,}} \quad \text{Eq. 4}$$

$$SCC_i = \Delta Temp_i + \alpha * \Delta pCO_{2_i} + \beta \quad \text{Eq. 5}$$

This synthetic temperature-$pCO_2$ axis, SCC, is centered on the ambient (control) conditions such that a value of 0 corresponds to present day Kāneʻohe Bay conditions, a negative value corresponds to water that is colder and less acidic (pre-industrial) and a positive value corresponds to water that is warmer and more acidic (future conditions) compared to background seawater. (The independent relationships between G and NCP

with ΔTemp and $\Delta pCO_2$ are shown in Figures A5 and A6 and are similar to the relationship with SCC.)

With SCC as a continuous, independent variable, we used a regression to test for linear and non-linear relationships between day, night, and net calcification ($G_{day}$, $G_{night}$, and $G_{net}$) and NCP ($NCP_{day}$, $NCP_{night}$, and $NCP_{net}$) versus SCC. For a simple test of nonlinearity in the response of calcification to SCC, we included a quadratic term ($SCC^2$) in the model. For $G_{day}$, we used weighted regression (weight function: $w_i=1/(1+|r_i|)$, where $w_i$ = weight and $r_i$ = residual, Fair, 1974) to account for heteroscedasticity. All other data met assumptions for a linear regression. Lastly, we used a linear regression to test the relationship between G and NCP.

# 3 Results

## 3.1 Control Experiment

For rubble in ambient seawater conditions, the average $G_{day}$, $G_{night}$, and $G_{net}$ in the control experiment were 3.4±0.16 mmol $m^{-2}$ $d^{-1}$, -2.4±0.15 mmol $m^{-2}$ $d^{-1}$, and 0.96±0.20 mmol $m^{-2}$ $d^{-1}$, respectively. There was no significant difference in $G_{day}$ ($F_{3,23}$=0.68, p=0.58), $G_{night}$ ($F_{3,23}$=1.52, p=0.24), or $G_{net}$ ($F_{3,23}$=1.38, p=0.28) between racks in the control experiment (Figure A2). NCP rates also did not show any racks effects. Average NCP rates were 23.2±1.4 mmol $m^{-2}$ $d^{-1}$ ($F_{3,23}$=0.07, p=0.94) during the day, -20.7±1.9 mmol $m^{-2}$ $d^{-1}$ ($F_{3,23}$=1.95, p=0.15) during the night, and 2.5±2.1 mmol $m^{-2}$ $d^{-1}$ ($F_{3,23}$=1.5, p=0.25) over the entire 24 hour period.

## 3.2 Treatment Experiment

The rubble communities significantly altered the seawater chemistry, with higher $pCO_2$ than the applied $pCO_2$ manipulation, particularly at night (Figure A1). The mean difference between day and night $pCO_2$ for all treatments was 134.4 ± 39 µatm without rubble and was 438.5 ± 163.9 µatm when rubble was present ($t_{23}$= -7.23, $p<0.0001$; Figure 2).

Standardized Climate Change was a significant predictor for $G_{day}$, $G_{night}$, and $G_{net}$ (Table 2; Figure 3). $G_{day}$ had a non-linear relationship with Standardized Climate Change (Table 2, Figure 3a), increasing to a threshold and then rapidly declining. $G_{night}$, however, had a strong linear relationship with Standardized Climate Change (Table 2; Figure 3c), suggesting that joint increases in ocean $pCO_2$ and temperature will increase nighttime dissolution of coral rubble. Lastly, $G_{net}$ had a strong negative relationship with Standardized Climate Change (Table 2; Figure 3e) and the rubble community switched from net calcification to net dissolution at an increase in $pCO_2$ and temperature of 271 µatm and 0.75° C, respectively. Standardized Climate Change was also a significant predictor of NCP: Day, night, and net NCP rates all declined with standardized climate change (Table 2; Figure 3b,d,f; Figure3).

Net ecosystem calcification increased with net community production ($F_{1,46}$ = 260, $p<0.0001$, $R^2$=0.85; Figure 4). In general, communities were net photosynthesizing and net calcifying during the day (Figure 4a: squares in the upper right quadrant) and were net respiring and net dissolving at night (Figure 4a: circles in the lower left quadrant). The exception was communities in the most extreme temperature-$pCO_2$

treatment: these communities were net respiring during the day while holding a positive, yet very low, calcification rate (Figure 4a: squares in the upper left quadrant).

# 4 Discussion

## 4.1 Carbonate Chemistry Feedbacks

The rubble communities in the aquaria significantly altered the seawater chemistry, particularly at night ($t_{23}$= -7.23, $p<0.0001$; Figure 2, Figure A1). This day-night difference in seawater chemistry increased under more extreme climate scenarios, as predicted by Jury *et al.* (2013). This large diel swing in $pCO_2$ is not uncommon on shallow coral reef environments. $pCO_2$ ranged from 480 to 975µatm over 24 hours on a shallow reef flat adjacent to our collection site (Silbiger et al. 2014) and from 450 to 742 µatm on a Moloka‘i reef flat dominated by coral rubble (Yates and Halley, 2006). Here, $pCO_2$ had an average difference of 438 µatm between day and night with a range of 412 µatm in the pre-industrial treatment to 854 µatm in the most extreme temperature-$pCO_2$ treatments (Figure 2). In our study, we incorporated these feedbacks into the statistical analysis by using the actual, sampled $pCO_2$ (and temperature) in each aquaria (Figure 3) rather than using the intended $pCO_2$ (and temperature) treatments in an ANOVA (Tables A1, A2 and Figures A3, A4), better reflecting the $pCO_2$ experienced by organisms in each aquarium.

## 4.2 Calcification, Dissolution, and Net Community Production in a High $CO_2$ and Temperature Environment

Our results suggest that as $pCO_2$ and temperature increase over time, rubble reefs may shift from net calcification to net dissolution. In our study, this tipping point occurred at a $pCO_2$ and temperature increase of 271 µatm and 0.75° C. Further, our results showed that $G_{day}$ and $G_{night}$ in a natural coral rubble community have different functional responses to changing $pCO_2$ and temperature (Figure 3). The ranges in $G_{day}$ and $G_{night}$ in our aquaria were similar to *in situ* rates on Hawaiian rubble reefs. Yates & Halley (2006) saw $G_{day}$ values between 3.3 to 11.7 mmol $CaCO_3$ $m^{-2}$ $d^{-1}$ and $G_{night}$ values between -2.4 to -24 mmol $CaCO_3$ $m^{-2}$ $d^{-1}$ on a Moloka‘i reef flat with only coral rubble (Note that Yates and Halley calculated G over a 4 hour timeframes and the data was multiplied by 3 here to show G in mmol $m^{-2}$ $d^{-1}$. Also note that we normalized our rates to the surface area of the rubble while Yates and Halley (2006) normalized their rates to planar surface area.). $G_{day}$ and $G_{night}$ in our experiment ranged from 1.9 to 9.4 and -1.3 to -10.5 mmol $CaCO_3$ $m^{-2}$ $d^{-1}$, respectively, across all treatment conditions. The higher dissolution rates in the *in situ* study by Yates and Halley (2006) are likely due to dissolution in the sediment, which was not present in our study.

$G_{day}$ had a non-linear response to Standardized Climate Change. $G_{day}$ increased with temperature-$pCO_2$ until slightly above ambient conditions, and then decreased under more extreme climate conditions (Figure 3a). This mixed response, increasing and then decreasing with Standardized Climate Change, is reflected in prior experiments. We suggest three possible mechanisms to explain why calcification increases in slightly higher temperature-$pCO_2$ than ambient conditions. 1) Some calcifiers can maintain and

392 even increase their calcification rates in acidic conditions (Kamenos et al., 2013;Findlay
393 et al., 2011;Rodolfo-Metalpa et al., 2011;Martin et al., 2013) by either modifying their
394 local pH environment (Hurd et al., 2011) or partitioning their energetic resources towards
395 calcification (Kamenos et al., 2013). For example, in low, stable pH conditions the
396 coralline algae, *Lithothamnion glaciale*, increased its calcification rate relative to a
397 control treatment but, did not concurrently increase its rate of photosynthesis (Kamenos
398 et al., 2013). Kamenos et al (2013) suggest that the up-regulation of calcification may
399 limit photosynthetic efficiency. In the present study, the increase in $G_{day}$ coincided with a
400 decrease in net photosynthesis (Figure 3a,b). Photosynthesizing calcifiers in the
401 community may be partitioning their energetic resources more towards calcification and
402 away from photosynthesis in order to maintain a positive calcification rate (Kamenos et
403 al., 2013). Notably, turf algae likely have a major control over the NCP in this
404 community which would not have any impact on calcification. 2) An alternative
405 hypothesis is that the calcifiers may be adapted or acclimatized to high $pCO_2$ conditions
406 (Johnson et al., 2014) and have not yet reached their threshold because the rubble was
407 collected from a naturally high and variable $pCO_2$ environment (Guadayol et al., 2014;
408 Silbiger et al. 2014). 3) In this study, the calcifiers experienced a combined increase in
409 both $pCO_2$ and temperature and, thus, the non-linear response in $G_{day}$ may also be due a
410 metabolic response. In a typical thermal performance curve, organisms increase their
411 metabolism until they have reached a thermal maximum and then rapidly decline (Huey
412 and Kingsolver, 1989; Pörtner et al., 2006), and we see this response in our results. A
413 recent study found a similar nonlinear response to temperature and $pCO_2$ in the coral
414 *Siderastrea sidera* (Castillo et al. 2014). While they attribute the $pCO_2$ response to

photosynthesis being neutralized (we did not see this response in our non-coral community), they suggest that the thermal response is due to both changes in metabolism and thermally-driven changes in aragonite saturation state (Castillo et al. 2014).

We saw a decline in both calcification and NCP in the extreme temperature-$pCO_2$ condition (Figure 3). Calcification has been shown to decline with climate stressors and the magnitude of decline differs across species (Kroeker et al., 2010;Pandolfi et al., 2011;Ries et al., 2009;Kroeker et al., 2013). The concurrent decline in NCP and calcification (Figure 3a,b & 4) suggests that non-photosynthesizing invertebrates in the community (such as bivalves) might be dominating the calcification signal in these conditions. This hypothesis would explain the pattern that we see in Figure 4, where communities in the most extreme $pCO_2$ and temperature conditions are net respiring during the day while still maintaining a small, positive calcification rate (Figure 4a: five points in the upper left quadrant).

$G_{night}$ rates are more straightforward, decreasing linearly with $pCO_2$ and temperature (Figures 3c and 4). $NCP_{night}$ rates also decreased linearly with $pCO_2$ and temperature (Figure 3d). Similarly, Andersson et al. (2009) saw an increase in dissolution under acidic conditions in a community of corals, sand, and CCA. Previous studies on individual bioeroder taxa have also found higher rates of bioerosion or dissolution in more acidic, higher temperature conditions (Wisshak et al., 2013;Fang et al., 2013;Reyes-Nivia et al., 2013;Tribollet et al., 2009;Wisshak et al., 2012). There are several mechanisms that could be mediating the increased dissolution rates in the high temperature-$pCO_2$ treatments: 1) Higher temperatures could increase the metabolism of the bioeroder community, thus increasing borer activity (e.g., Davidson et al. 2013). 2)

Because many boring organisms excrete acidic compounds to erode the skeletal structure (Hutchings 1986), reduced pH in the overlaying water column may reduce the metabolic cost to the organisms, making it easier for eroders to breakdown the $CaCO_3$. 3) Higher dissolution rates could be mediated by an increase in the proportion of dolomite in the skeletal structure of CCA on the rubble. A recent study found a 200% increase in dolomite in CCA that was exposed to high $pCO_2$ and temperature conditions; this increase in dolomite resulted in increased bioerosion by endolithic algae (Diaz-Pulido et al., 2014). However, it is unlikely that changes in the mineralogy of the CCA indirectly increased dissolution here given the short time-scale of our study. In the present study, we used the TA anomaly method to calculate chemical dissolution as a proxy for bioerosion. Future studies should also include measures of mechanical breakdown (e.g. the production of sponge chips) in addition to chemical dissolution for a more complete picture of the impacts of climate stress on reef breakdown. Studies, including the present one, which focused on community-level responses, have consistently found that ocean acidification will increase dissolution rates on coral reefs (Andersson and Gledhill, 2013).

Standardized Climate Change explained more of the variance in dissolution than in calcification in our rubble community: ($R^2_{G_{night}} = 0.64 > R^2_{G_{day}} = 0.33$; Table 2) this result is not surprising. Bioerosion, an important driver of dissolution, may be more sensitive to changes in ocean acidity than calcification, leading to net dissolution in high $CO_2$ waters. Many boring organisms excrete acidic compounds, which may be less metabolically costly in a low pH environment. Erez et al. (2011) hypothesize that increased dissolution, rather than decreased calcification, maybe be the reason that net

460 coral reef calcification is sensitive to ocean acidification. The results of this study support
461 this hypothesis. Although $G_{net}$ declines linearly with $pCO_2$-temperature, calcification
462 ($G_{day}$) and dissolution ($G_{night}$) have distinct responses to Standardized Climate Change:
463 $G_{day}$ had a non-linear response while $G_{night}$ declined linearly with Standardized Climate
464 Change. Our results highlight the need to study the effects of climate stressors on both
465 calcification and dissolution.

466 **Author contributions**:

467 Conceived and designed the experiments: NJS MJD. Performed the experiments: NJS.
468 Analyzed the data: NJS MJD. Wrote the paper: NJS MJD.

469 **Acknowledgements**

470 Thanks to I Caldwell, R Coleman, J Faith, K Hurley, J Miyano, R Maguire, D. Schar, JM
471 Sziklay, and MM Walton for help in field collections and lab analyses and to R. Briggs
472 from UH SOEST Lab for Analytical Chemistry. MJ Atkinson, R. Gates, C Jury, H
473 Putnam, and R Toonen gave thoughtful advice throughout the project. Comments by F.
474 Mackenzie and our two anonymous reviewers improved this manuscript. This project
475 was supported by a NOAA Dr. Nancy Foster Scholarship to N.J.S., a PADI Foundation
476 Grant to N.J.S., and Hawaii SeaGrant 1847 to MJD. This paper is funded in part by a
477 grant /cooperative agreement from the National Oceanic and Atmospheric
478 Administration, Project R/IR-18, which is sponsored by the University of Hawaii Sea
479 Grant College Program, SOEST, under Institutional Grant No. NA09OAR4170060 from
480 NOAA Office of Sea Grant, Department of Commerce. The views expressed herein are
481 those of the author(s) and do not necessarily reflect the views of NOAA or any of its

482 subagencies. This is HIMB contribution #1607, Hawai‘i SeaGrant contribution # UNIHI-
483 SEAGRANT-JC-12-19, and SOEST #9237.
484

## References


Adey, W.H. Review—coral reefs: algal structures and mediated ecosystems in shallow turbulent, alkaline waters. Journal of Phycology, 34, 393-406, 1998.

Andersson, A. J., Kuffner, I. B., Mackenzie, F. T., Jokiel, P. L., Rodgers, K. S., and Tan, A.: Net Loss of $CaCO_3$ from a subtropical calcifying community due to seawater acidification: mesocosm-scale experimental evidence, Biogeosciences, 6, 1811-1823, 2009.

Andersson, A. J., Mackenzie, F. T., and Gattuso, J.-P.: Effects of ocean acidification on benthic processes, organisms, and ecosystems, in: Ocean Acidification, edited by: Gattuso, J.-P., and Hansson, L., Oxford University Press, 122-153, 2011.

Andersson, A. J., and Mackenzie, F. T.: Revisiting four scientific debates in ocean acidification research, Biogeosciences, 9, 893-905, 2012.

Andersson, A. J., and Gledhill, D.: Ocean Acidification and Coral Reefs: Effects on Breakdown, Dissolution, and Net Ecosystem Calcification, Annual Review of Marine Science, Vol 5, 5, 321-348, 2013.

Bopp, L., Resplandy, L., Orr, J. C., Doney, S. C., Dunne, J. P., Gehlen, M., Halloran, P., Heinze, C., Ilyina, T., Séférian, R., Tjiputra, J., and Vichi, M.: Multiple stressors of ocean ecosystems in the 21st century: projections with CMIP5 models, Biogeosciences, 10, 3627-3676, 2013.

Caldeira, K., and Wickett, M. E.: Oceanography: anthropogenic carbon and ocean pH, Nature, 425, 365-365, 2003.

Camoin, G.F., Montaggioni, L.F., High energy coralgal-stromatolite frameworks from Holocene reefs (Tahiti, French Polynesia), Sedimentology, 41, 656-676, 1994.

Castillo, K.D., Ries, J.B., Bruno, J.F., Westfield, I.T., The reef-building coral *Siderastrea siderea* exhibits parabolic responses to ocean acidification and warming. Proc. R. Soc. B., 281, 20141856, 2014

Comeau, S., Edmunds, P. J., Spindel, N. B., and Carpenter, R. C.: The responses of eight coral reef calcifiers to increasing partial pressure of $CO_2$ do not exhibit a tipping point, Limnol. Oceanogr, 58, 388-398, 2013.

Cubasch, U., Wuebbles, D., Chen, D., Facchini, M. C., Frame, D., Mahowald, N., and Winther, J.-G.: Climate Change 2013: The Physical Science Basis. Contribution of Working Group I to the Fifth Assessment Report of the Intergovernmental Panel on Climate Change Cambridge, United Kingdom and New York, NY, USA. , 2013.

Davidson, T.M., de Rivera, C.E., Carlton, J.T., Small increases in temperature exacerbate the erosive effects of a non-native burrowing crustacean, Journal of Experimenal Marine Biology and Ecology, 446, 115-121, 2013.

Diaz-Pulido, G., Anthony, K., Kline, D. I., Dove, S., and Hoegh-Guldberg, O.: Interactions between ocean acidification and warming on the mortality and dissolution of coralline alge, Journal of Phycology, 48, 32-39, 2012.

524 Diaz-Pulido, G., Nash, M.C., Anthony, K.R.N., Bender. D., Opdyke, B.N., Reyed-Nivia,
525 C., Troitzsch, U., Greenhouse conditions induce mineralogical changes and dolomite
526 accumulation in coralline algae on tropical reefs, Nature Communications, 5, 3310,
527 DOI:10.1038/ncomms4310, 2014

528 Dickson, A. G., and Millero, F. J.: A comparison of the equilibrium constants for the
529 dissociation of carbonic acid in seawater media, Deep Sea Research Part A.
530 Oceanographic Research Papers, 34, 1733-1743, 1987.

531 Dickson, A. G.: Standard potential of the reaction: AgCl (s)+ $12H_2$(g)= Ag (s)+ HCl (aq),
532 and and the standard acidity constant of the ion $HSO_4^-$ in synthetic sea water from 273.15
533 to 318.15 K, The Journal of Chemical Thermodynamics, 22, 113-127, 1990.

534 Dickson, A. G., Sabine, C. L., and Christian, J. R.: Guide to best practices for ocean CO2
535 measurements, 2007.

536 Doney, S. C., Fabry, V. J., Feely, R. A., and Kleypas, J. A.: Ocean Acidification: The
537 Other $CO_2$ Problem, Annual Review of Marine Science, 1, 169-192, 2009.

538 Drupp, P. S., De Carlo, E. H., Mackenzie, F. T., Sabine, C. L., Feely, R. A., and
539 Shamberger, K. E.: Comparison of $CO_2$ dynamics and air–sea gas exchange in differing
540 tropical reef environments, Aquatic Geochemistry, 19, 371-397, 2013.

541 Erez, J., Reynaud, S., Silverman, J., Schneider, K., and Allemand, D.: Coral calcification
542 under ocean acidification and global change, in: Coral Reefs: an ecosystem in transition,
543 edited by: Dubinski, Z., and Stambler, N., Springer, 2011.

544 Fabricius, K., Langdon, C., Uthicke, S., Humphrey, C., Noonan, S., De'ath, G., Okazaki,
545 R., Muehllehner, N., Glas, M., and Lough, J.: Losers and winners in coral reefs
546 acclimatized to elevated carbon dioxide concentrations, Nature Climate Change, 1, 165-
547 169, 2011.

548 Fabricius, K. E.: Effects of terrestrial runoff on the ecology of corals and coral reefs:
549 review and synthesis, Mar. Pollut. Bull., 50, 125-146, 2005.

550 Fair, R. C.: On the robust estimation of econometric models, in: Annals of Economic and
551 Social Measurement, Volume 3, number 4, NBER, 117-128, 1974.

552 Fang, J. K. H., Mello-Athayde, M. A., Schönberg, C. H. L., Kline, D. I., Hoegh-
553 Guldberg, O., and Dove, S.: Sponge biomass and bioerosion rates increase under ocean
554 warming and acidification, Global Change Biology, 19, 3581-3591, 2013.

555 Fangue, N. A., O'Donnell, M. J., Sewell, M. A., Matson, P. G., MacPherson, A. C., and
556 Hofmann, G. E.: A laboratory-based, experimental system for the study of ocean
557 acidification effects on marine invertebrate larvae, Limnology and Oceanography:
558 Methods, 8, 441-452, 2010.

559 Feely, R. A., Sabine, C. L., Lee, K., Berelson, W., Kleypas, J., Fabry, V. J., and Millero,
560 F. J.: Impact of anthropogenic $CO_2$ on the $CaCO_3$ system in the oceans, Science, 305,
561 362-366, 2004.

562 Findlay, H. S., Wood, H. L., Kendall, M. A., Spicer, J. I., Twitchett, R. J., and
563 Widdicombe, S.: Comparing the impact of high $CO_2$ on calcium carbonate structures in
564 different marine organisms, Marine Biology Research, 7, 565-575, 2011.

565 Gattuso, J.-P., Frankignoulle, M., and Smith, S. V.: Measurement of community
566 metabolism and significance in the coral reef $CO_2$ source-sink debate, Proceedings of the
567 National Academy of Sciences, 96, 13017-13022, 1999.

568 Guadayol, Ò., Silbiger, N. J., Donahue, M. J., and Thomas, F. I. M.: Patterns in Temporal
569 Variability of Temperature, Oxygen and pH along an Environmental Gradient in a Coral
570 Reef, PloS one, 9, e85213, DOI:10..1371/journal.pone.0085213, 2014.

571 Harrington, L., Fabricius, K., De'ath, G., Negri, A., Recognition and selection of
572 settlement substrata determine post-settlement survival in corals. Ecology, 84-3428-3437,
573 2004.

574 Hoegh-Guldberg, O., Mumby, P. J., Hooten, A. J., Steneck, R. S., Greenfield, P., Gomez,
575 E., Harvell, C. D., Sale, P. F., Edwards, A. J., Caldeira, K., Knowlton, N., Eakin, C. M.,
576 Iglesias-Prieto, R., Muthiga, N., Bradbury, R. H., Dubi, A., and Hatziolos, M. E.: Coral
577 reefs under rapid climate change and ocean acidification, Science, 318, 1737-1742, 2007.

578 Huey, R.B., Kingsolver, J.G. Evolution of thermal sensitivity of ecotherm performance.
579 Trends Ecol. Evol., 4,131-135, 1989

580 Hutchings, P.A., Biological destruction of coral reefs, Coral Reefs, 4, 239-252, 1986.

581 Hoegh-Guldberg, O., and Bruno, J. F.: The impact of climate change on the world's
582 marine ecosystems, Science, 328, 1523-1528, 2010.

583 Hurd, C. L., Cornwall, C. E., Currie, K., Hepburn, C. D., McGraw, C. M., Hunter, K. A.,
584 and Boyd, P. W.: Metabolically induced pH fluctuations by some coastal calcifiers
585 exceed projected 22nd century ocean acidification: a mechanism for differential
586 susceptibility?, Global Change Biology, 17, 3254-3262, 2011.

587 Johnson, M. D., and Carpenter, R. C.: Ocean acidification and warming decrease
588 calcification in the crustose coralline alga *Hydrolithon onkodes* and increase
589 susceptibility to grazing, J. Exp. Mar. Biol. Ecol., 434, 94-101, 2012.

590 Johnson, M. D., Moriarty, V. W., and Carpenter, R. C.: Acclimatization of the Crustose
591 Coralline Alga *Porolithon onkodes* to Variable $pCO_2$, PLOS ONE, 9, e87678, DOI:
592 10.1371/journal.pone.0087678, 2014.

593 Jokiel, P. L., Rodgers, K. S., Kuffner, I. B., Andersson, A. J., Cox, E. F., and Mackenzie,
594 F. T.: Ocean acidification and calcifying reef organisms: a mesocosm investigation, Coral
595 Reefs, 27, 473-483, 2008.

596 Jury, C. P., Thomas, F. I. M., Atkinson, M. J., and Toonen, R. J.: Buffer Capacity,
597 Ecosystem Feedbacks, and Seawater Chemistry under Global Change, Water, 5, 1303-
598 1325, 2013.

599 Kamenos, N. A., Burdett, H. L., Aloisio, E., Findlay, H. S., Martin, S., Longbone, C.,
600 Dunn, J., Widdicombe, S., and Calosi, P.: Coralline algal structure is more sensitive to

601 rate, rather than the magnitude, of ocean acidification, Global Change Biology, 19, 3621-
602 3628, 2013.

603 Kleypas, J., and Langdon, C.: Coral reefs and changing seawater chemistry, in: Coral
604 Reefs and Climate Change: Science and Management., edited by: Phinney, J., Skirving,
605 W., Kleypas, J., and Hoegh-Guldberg, O., American Geophysical Union, Washington
606 D.C., pp. 73-110, 2006.

607 Kroeker, K. J., Kordas, R. L., Crim, R. N., and Singh, G. G.: Meta-analysis reveals
608 negative yet variable effects of ocean acidification on marine organisms, Ecology Letters,
609 13, 1419-1434, 2010.

610 Kroeker, K. J., Kordas, R. L., Crim, R., Hendriks, I. E., Ramajo, L., Singh, G. S., Duarte,
611 C. M., and Gattuso, J. P.: Impacts of ocean acidification on marine organisms:
612 quantifying sensitivities and interaction with warming, Global Change Biology, 19, 1884-
613 1896, 2013.

614 Littler, M.M.m The population and community structure of Hawaiian fringing-reef
615 crustose corallinaceae (Rhodophyta, Cryptonemiales), Journal of Experimental Marine
616 Biology and Ecology, 11, 103-120, 1973.

617 Lowe, R. J., Falter, J. L., Monismith, S. G., and Atkinson, M. J.: A numerical study of
618 circulation in a coastal reef-lagoon system, Journal of Geophysical Research-Oceans,
619 114, C06022, 2009a.

620 Lowe, R. J., Falter, J. L., Monismith, S. G., and Atkinson, M. J.: Wave-driven circulation
621 of a coastal reef-lagoon system, J. Phys. Oceanogr., 39, 873-893, 2009b.

622 Martin, S., Cohu, S., Vignot, C., Zimmerman, G., and Gattuso, J. P.: One-year
623 experiment on the physiological response of the Mediterranean crustose coralline alga,
624 *Lithophyllum cabiochae*, to elevated $pCO_2$ and temperature, Ecology and evolution, DOI:
625 10.1029/2008JC005081, 2013.

626 Mehrbach, C.: Measurement of the apparent dissociation constants of carbonic acid in
627 seawater at atmospheric pressure, Limnol. Oceanogr., 18, 897-907, 1973.

628 Meinshausen, M., Smith, S. J., Calvin, K., Daniel, J. S., Kainuma, M. L. T., Lamarque, J.
629 F., Matsumoto, K., Montzka, S. A., Raper, S. C. B., and Riahi, K.: The RCP greenhouse
630 gas concentrations and their extensions from 1765 to 2300, Climatic Change, 109, 213-
631 241, 2011.

632 Pandolfi, J. M., Connolly, S. R., Marshall, D. J., and Cohen, A. L.: Projecting coral reef
633 futures under global warming and ocean acidification, Science, 333, 418-422, 2011.

634 Price, N., Habitat selection, facilitation, and biotic settlement cues affect distribution and
635 performance of coral recruits in French Polynesia, Oecologia, 163, 747-758, 2010.

636 Pörtner, H.O., Bennet, A.F., Bozinovic, F., Clarke, A., Lardies, M.A., Lucassen, M.,
637 Pelster, B., Schiemer, F., Stillman, J.H., Trade-offs in therman adaptation: the need for
638 molecular ecological integration, Phys. Biochem. Zool., 79, 295-313, 2006.

639 Putnam, H.M. Resilience and acclimitization potential of reef corals under predicted
640 climate change stressors, PhD, Zoology, University of Hawaii at Manoa, Honolulu, 2012

Reyes-Nivia, C., Diaz-Pulido, G., Kline, D., Guldberg, O.-H., and Dove, S.: Ocean acidification and warming scenarios increase microbioerosion of coral skeletons, Global Change Biology, 19, 1919-1929, 2013.

Ries, J. B., Cohen, A. L., and McCorkle, D. C.: Marine calcifiers exhibit mixed responses to $CO_2$-induced ocean acidification, Geology, 37, 1131-1134, 2009.

Rodolfo-Metalpa, R., Houlbrèque, F., Tambutté, É., Boisson, F., Baggini, C., Patti, F. P., Jeffree, R., Fine, M., Foggo, A., and Gattuso, J. P.: Coral and mollusc resistance to ocean acidification adversely affected by warming, Nature Climate Change, 1, 308-312, 2011.

Rogelj, J., Meinshausen, M., and Knutti, R.: Global warming under old and new scenarios using IPCC climate sensitivity range estimates, Nature Climate Change, 2, 248-253, 2012.

Sanford, T., Frumhoff, P. C., Luers, A., and Gulledge, J.: The climate policy narrative for a dangerously warming world, Nature Climate Change, 4, 164-166, 2014.

Semesi, I. S., Kangwe, J., and Björk, M.: Alterations in seawater pH and $CO_2$ affect calcification and photosynthesis in the tropical coralline alga, *Hydrolithon* sp.(Rhodophyta), Estuarine, Coastal and Shelf Science, 84, 337-341, 2009.

Silbiger, N., Guadayol, Ò., Thomas, F. I., and Donahue, M.: Reefs shift from net accretion to net erosion along a natural environmental gradient, Marine Ecology Progress Series, 515, 33-44, 2014.

Smith, S. V., and Key, G. S.: Carbon dioxide and metabolism in marine environments, Limnol. Oceanogr, 20, 493-495, 1975.

Smith, S. V., Kimmerer, W. J., Laws, E. A., Brock, R. E., and Walsh, T. W.: Kaneohe Bay sewage diversion experiment- perspectives on ecosystem responses to nutritional perturbation, Pacific Science, 35, 279-402, 1981.

Solomon, S., Qin. D., Manning. M. Chen. Z., Marquis, M., et al. Climate Change 2007: The physical Science Basis: Contributions of Working Group I to the Fourth Assessment Report of the Intergovernmental Panel on Climate Change., New York, Cambridge Univ. Press, 2007.

Stimson, J., and Kinzie III, R. A.: The temporal pattern and rate of release of zooxanthellae from the reef coral *Pocillopora damicornis* (Linnaeus) under nitrogen-enrichment and control conditions, Journal of Experimental Marine Biology and Ecology, 153, 63-74, 1991.

Tans, P., and Keeling, R.: NOAA/ESRL, www.esrl.noaa.gov/gmd/ccgg/trends/, 2013.

Tribollet, A., and Payri, C.: Bioerosion of the coralline alga *Hydrolithon onkodes* by microborers in the coral reefs of Moorea, French Polynesia, Oceanologica Acta, 24, 329-342, 2001.

Tribollet, A., Atkinson, M. J., and Langdon, C.: Effects of elevated $pCO_{(2)}$ on epilithic and endolithic metabolism of reef carbonates, Global Change Biology, 12, 2200-2208, 2006.

680 Tribollet, A., Godinot, C., Atkinson, M., and Langdon, C.: Effects of elevated $pCO_{(2)}$ on
681 dissolution of coral carbonates by microbial euendoliths, Global Biogeochemical Cycles,
682 23, GB3008, 2009.

683 Uppström, L. R.: The boron/chlorinity ratio of deep-sea water from the Pacific Ocean,
684 Deep Sea Research and Oceanographic Abstracts, 1974, 161-162.

685 Van Heuven, S., Pierrot, D., Lewis, E., and Wallace, D. W. R.: MATLAB Program
686 developed for CO2 system calculations, Rep. ORNL/CDIAC-105b, 2009.

687 Van Vuuren, D. P., Meinshausen, M., Plattner, G. K., Joos, F., Strassmann, K. M., Smith,
688 S. J., Wigley, T. M. L., Raper, S. C. B., Riahi, K., and De La Chesnaye, F.: Temperature
689 increase of 21st century mitigation scenarios, Proceedings of the National Academy of
690 Sciences, 105, 15258-15262, 2008.

691 Van Vuuren, D. P., Edmonds, J., Kainuma, M., Riahi, K., Thomson, A., Hibbard, K.,
692 Hurtt, G. C., Kram, T., Krey, V., and Lamarque, J.-F.: The representative concentration
693 pathways: an overview, Climatic Change, 109, 5-31, 2011.

694 White, J.: Distribution, recruitment and development of the borer community in dead
695 coral on shallow Hawaiian reefs, Ph.D., Zoology, University of Hawaii at Manoa,
696 Honolulu, 1980.

697 Wisshak, M., Schönberg, C. H. L., Form, A., and Freiwald, A.: Ocean acidification
698 accelerates reef bioerosion, Plos One, 7, e45124-e45124, 2012.

699 Wisshak, M., Schönberg, C. H. L., Form, A., and Freiwald, A.: Effects of ocean
700 acidification and global warming on reef bioerosion—lessons from a clionaid sponge,
701 Aquatic Biology, 19, 111-127, 2013.

702 Wolf-Gladrow, D.A., Zeebe, R.E., Klass, C., Körtzinger, A., Dickson, A.G.,: Total
703 Alkalinity: The explicit conservative expression and its application to biogeochemical
704 processes, Marine Chemistry, 106, 287-300, 2007.

705 Yates, K. K., and Halley, R. B.: $CO_3^{2-}$ concentration and $pCO_2$ thresholds for calcification
706 and dissolution on the Molokai reef flat, Hawaii, Biogeosciences, 3, 357-369, 2006.

707

Table 1: Means and standard errors of all measured parameters by rack. $pCO_2$, $HCO_3^-$, $CO_3^{2-}$, DIC, and $\Omega_{arag}$ were all calculated from the measured TA and pH samples using CO2SYS. Each table entry is the mean of 12 water samples: one daytime sample and one nighttime sample for six aquaria within a rack. Data are all from the imposed treatment conditions with no rubble inside the aquaria.

| **Rack** | **Pre-industrial** | **Present Day** | **2050 prediction** | **2100 prediction** |
|---|---|---|---|---|
| **Temp (°C)** | 23.8±0.07 | 24.8±0.08 | 26.2±0.06 | 27.2±0.08 |
| **Salinity(psu)** | 35.65±0.01 | 35.71±0.02 | 35.62±0.02 | 35.71±0.02 |
| **Total Alkalinity (µmol $kg^{-1}$)** | 2137±1.7 | 2138±2.3 | 2139±2.0 | 2142±1.9 |
| **$pH_t$** | 8.02±0.02 | 7.87±0.01 | 7.74±0.02 | 7.67±0.02 |
| **$pCO_2$ (µatm)** | 409±20.0 | 614±15.6 | 868±33.0 | 1047±38.7 |
| **$HCO_3^-$ (µmol $kg^{-1}$)** | 1692±16.9 | 1815±7.3 | 1894±7.8 | 1939±6.6 |
| **$CO_3^{2-}$ (µmol $kg^{-1}$)** | 194.20±6.7 | 147.08±2.8 | 113.98±3.8 | 99.24±3.3 |
| **DIC (µmol $kg^{-1}$)** | 1898±10.9 | 1980±5.1 | 2032±5.0 | 2067±4.5 |
| **$\Omega_{arag}$** | 3.06±0.1 | 2.32±0.04 | 1.80±0.06 | 1.57±0.05 |
| **$NO_2^-$ (µmol $L^{-1}$)** | 0.082 ± 0.0028 | 0.078 ±0.0045 | 0.074 ± 0.0047 | 0.070 ± 0.0051 |
| **$PO_4^{3-}$ (µmol $L^{-1}$)** | 0.017 ±0.014 | 0.0097 ±0.0081 | 0.033 ±0.016 | 0.018±0.0061 |
| **$Si(OH)_4$ (µmol $L^{-1}$)** | 3.60 ±0.58 | 3.64 ±0.61 | 3.88 ± 0.49 | 3.78 ± 0.52 |
| **$NH_4^+$ (µmol $L^{-1}$)** | 0.45 ±0.30 | 0.19 ±0.067 | 0.23 ±0.15 | 0.34 ± 0.14 |
| **$NO_3^-$(µmol $L^{-1}$)** | 2.13±0.20 | 2.25±0.21 | 2.55±0.10 | 2.48±0.11 |

711 Table 2: Regression results for the treatment experiments: $G_{day}$, $G_{night}$, and $G_{net}$ versus
712 Standardized Climate Change (Figure 3a,c,e) and $NCP_{day}$, $NCP_{night}$, and $NCP_{net}$ versus
713 Standardized Climate Change (Figure 3b,d,f). Bold values indicate a statistically significant
714 p-value at an $\alpha < 0.05$.

| | SS | df | F | p | $R^2$ |
|---|---|---|---|---|---|
| **$G_{day}$** | | | | | |
| Standardized Climate Change | 3.79 | 1 | 1.45 | 0.06 | |
| (Standardized Climate Change)$^2$ | 23.63 | 1 | 9.04 | **0.007** | |
| Error | 54.89 | 21 | | | 0.33 |
| **$G_{night}$** | | | | | |
| Standardized Climate Change | 67.80 | 1 | 39.14 | **<0.0001** | |
| Error | 38.11 | 22 | | | 0.64 |
| **$G_{net}$** | | | | | |
| Standardized Climate Change | 88.01 | 1 | 19.49 | **<0.001** | |
| Error | 99.35 | 22 | | | 0.47 |
| **$NCP_{day}$** | | | | | |
| Standardized Climate Change | 5687.2 | 1 | 57.36 | **<0.0001** | |
| Error | 2181.4 | 22 | | | 0.72 |
| **$NCP_{night}$** | | | | | |
| Standardized Climate Change | 3816.1 | 1 | 52.06 | **<0.0001** | |
| Error | 1612.6 | 22 | | | 0.70 |
| **$NCP_{net}$** | | | | | |
| Standardized Climate Change | 17925 | 1 | 121.47 | **<0.0001** | |
| Error | 3246.4 | 22 | | | 0.85 |

715

716

## Figure legends:

**Figure 1:** A schematic of the mesocosm system at the Hawai‘i Institute of Marine Biology. Ambient seawater is pumped into the system from a nearby fringing reef in Kāne‘ohe Bay. The seawater is filtered with a sand trap filter, passed through a water chiller and then fed into one of four header tanks. $pCO_2$ is manipulated in each header tank by bubbling a mixture of $CO_2$-free air and pure $CO_2$ to the desired concentration. The water from one header tank flows into 6 aquaria (a rack). Light is controlled by rack with metal-halide lights. There are two metal-halide lights per rack with each light oscillating over a set of three aquaria. Flow and temperature are controlled in each individual aquarium with flow valves and aquarium heaters and coolers, respectively.

**Figure 2:** $pCO_2$ and temperature in each aquarium (a) without any rubble present and (b) with rubble present. Daily variability in $pCO_2$ was higher when rubble was present due to feedbacks from the rubble community (note the different x-axis scales in panels a and b). Panel (c) shows the mean difference between day and night $pCO_2$ with and without rubble present with observations paired by aquarium (error bars are standard error) ($t_{23}$= -7.23, $p<0.0001$).

**Figure 3:** Net ecosystem calcification ( (a) $G_{day}$, (c) $G_{night}$, (e) and $G_{net}$) and net community production ( (b) $NCP_{day}$, (d) $NCP_{night}$, and (f) $NCP_{net}$) versus Standardized Climate Change (SCC). Each point represents net ecosystem calcification (left panel) or net community production (right panel) calculated from an individual aquarium. Standardized Climate Change was centered around background seawater conditions such that a value of 0 indicated that there was no change in $pCO_2$ or temperature. Positive values indicate an elevated $pCO_2$ and temperature condition relative to background and negative values represent lower $pCO_2$ and temperature conditions. $G_{day}$ had a non-linear relationship with Standardized Climate

Change ($y$ = -0.27 $x^2$ + 0.59$x$+5.7), while $G_{night}$ ($y$=-0.63$x$ - 3.6) and $G_{net}$ ($y$=--0.76$x$ + 1.1) each had a negative linear relationship with Standardized Climate Change (Table 2). $NCP_{day}$ ($y$=-7.01$x$ +23.4), $NCP_{night}$ ($y$=-35.76 – 4.74), and $NCP_{net}$ ($y$=-12.07$x$ – 10.85) all had significant negative relationships with Standardized Climate Change. Black lines are best fit lines for each model with 95% confidence intervals in gray. Greek letters on the top panel represent the imposed conditions for pre-industrial (α), Present Day (β), 2050 (γ), and 2100(δ). The black horizontal line in in panels (b), (e) and (f) shows the point where G and NCP = 0. Points above the line are net calcifying (e) or net photosynethsizing (f) and points below the line are net dissolving (e) or net respiring (f) over the entire 24 hour period.

**Figure 4**: (a) Calculated G and NCP rates for all treatment aquaria. Squares are data collected during light (day) conditions and circles represent data collected during dark (night) conditions, and the color represents Standardized Climate Change (color bar). There is a strong positive relationship between G and NCP ($y$ = 0.14$x$ + 1.9, $p<0.0001$, $R^2=0.85$). Negative and positive y-values are net dissolution and net calcification, respectively; negative and positive x-values are net respiration and net photosynthesis, respectively. (b) TA versus DIC: There is a strong positive relationship between TA and DIC ($y$ = 0.31$x$ + 1577.4, $p<0.0001$, $R^2=0.85$). Black and gray lines represent the best-fit line and 95% confidence intervals, respectively. As expected, the slope of TA versus DIC (0.31) is approximately twice that of G versus NCP (0.14).

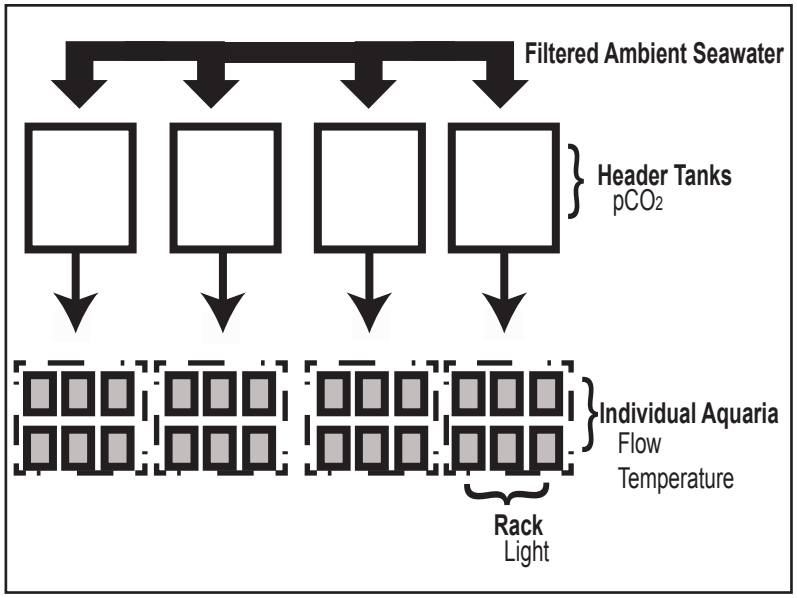
Filtered Ambient Seawater
Header Tanks
pCO2
Individual Aquaria
Flow
Temperature
Rack
Light

Figure 1

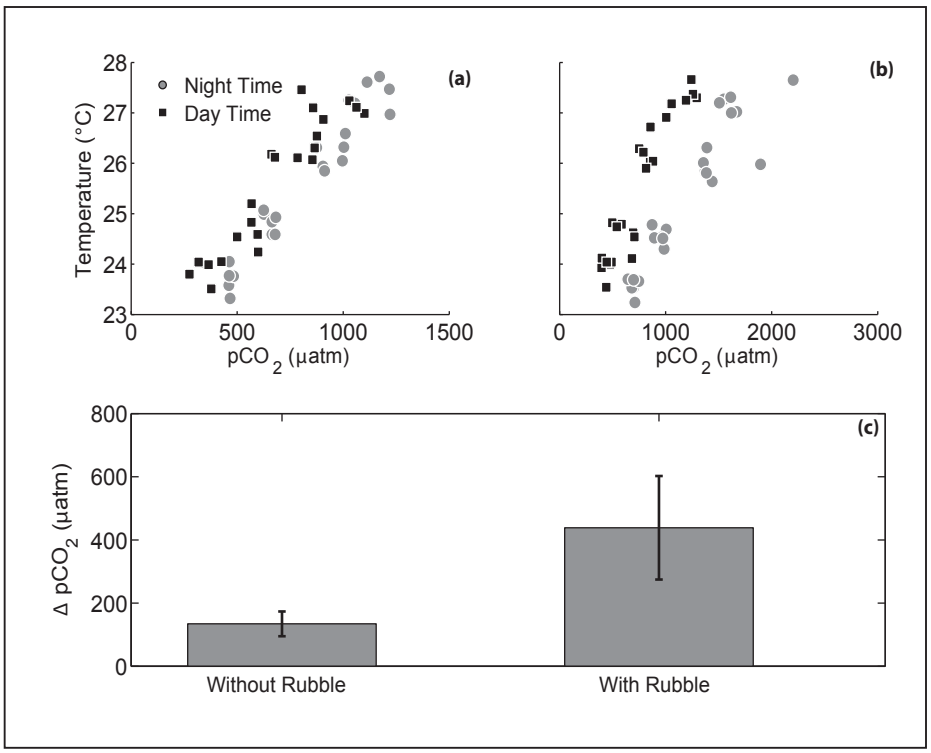
(a)
Night Time
Day Time
Temperature (°C)
28
27
26
25
24
23
0
500
1000
1500
pCO 2 (µatm)
(b)
0
1000
2000
3000
pCO 2 (µatm)
(c)
Δ pCO2 (µatm)
800
600
400
200
0
Without Rubble
With Rubble

Figure 2

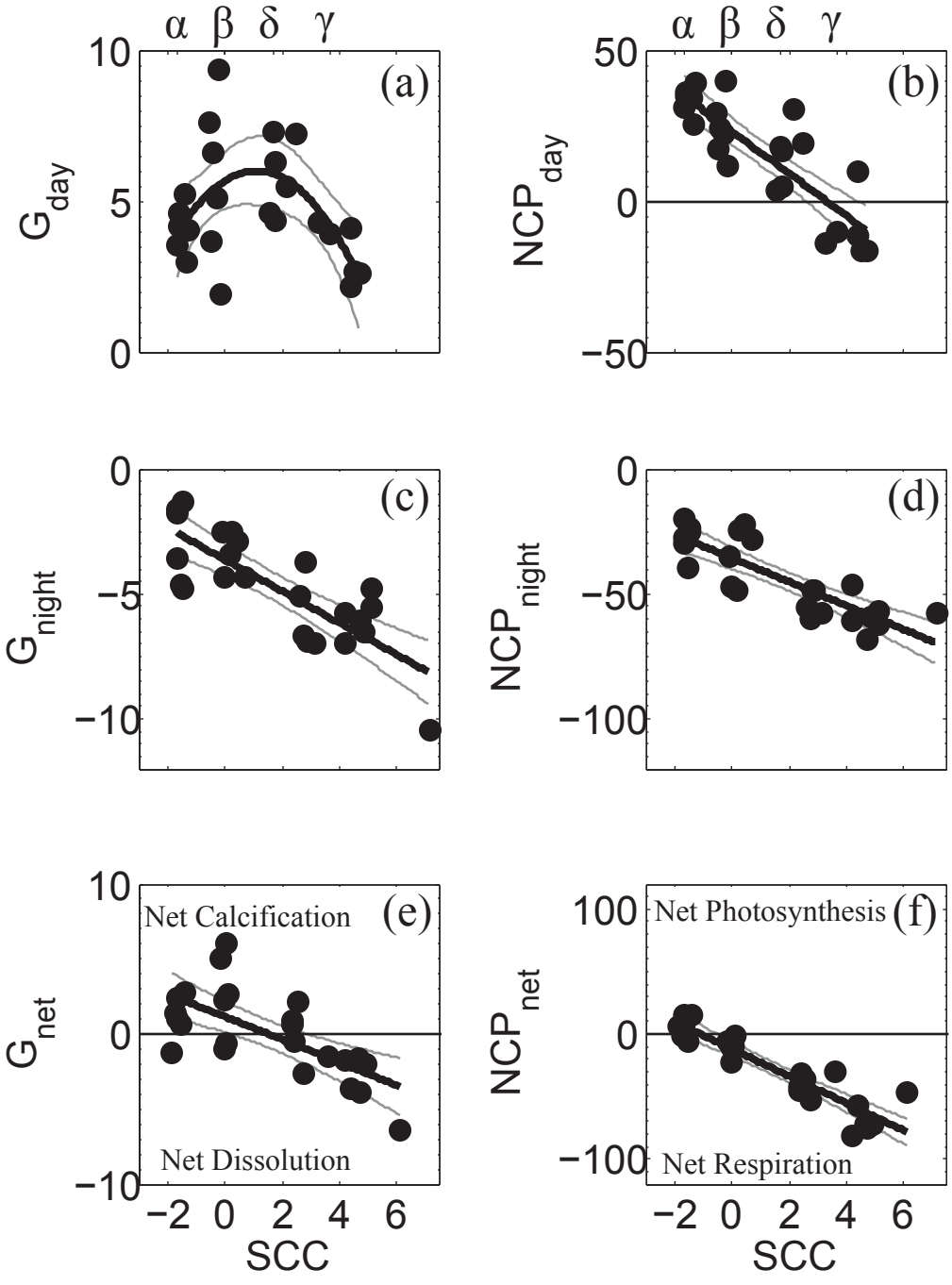
α β δ γ
(a)
$G_{day}$
10
5
0
α β δ γ
(b)
$NCP_{day}$
50
0
−50
(c)
$G_{night}$
0
−5
−10
(d)
$NCP_{night}$
0
−50
−100
(e)
Net Calcification
Net Dissolution
$G_{net}$
10
0
−10
−2 0 2 4 6
SCC
(f)
Net Photosynthesis
Net Respiration
$NCP_{net}$
100
0
−100
−2 0 2 4 6
SCC

Figure 3

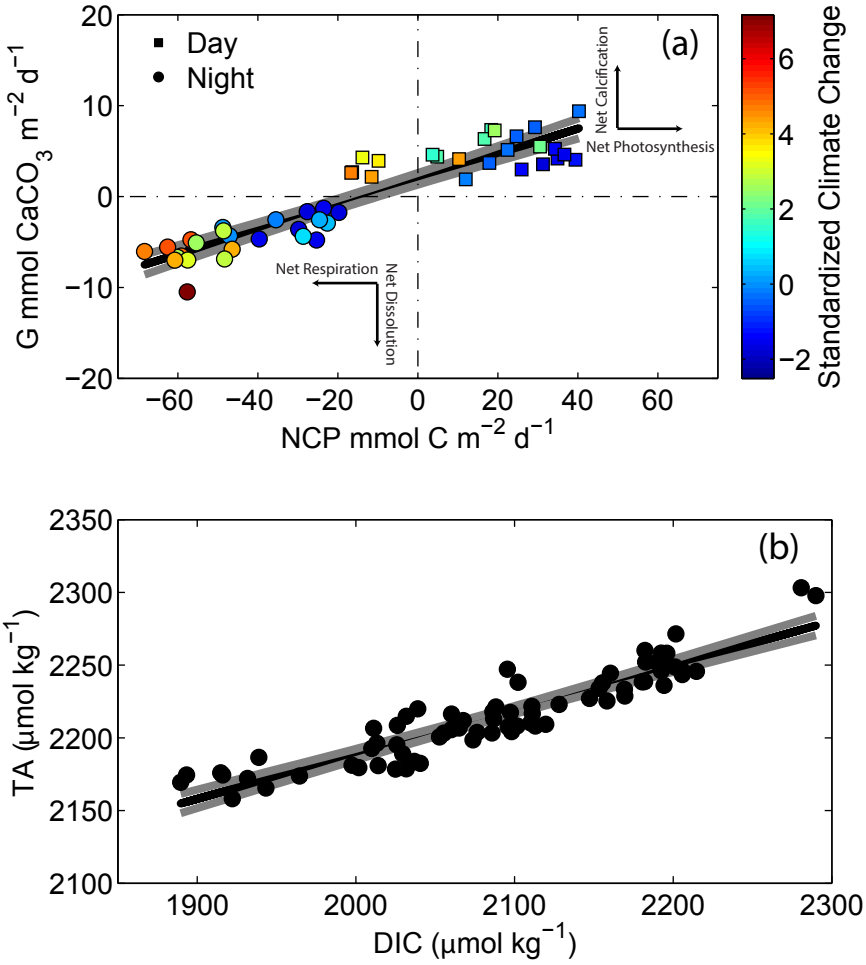
(a)
Day
Night
Net Calcification
Net Photosynthesis
Net Respiration
Net Dissolution
G mmol CaCO3 m−2 d−1
NCP mmol C m−2 d−1
Standardized Climate Change
20
10
0
−10
−20
−60
−40
−20
0
20
40
60
6
4
2
0
−2
(b)
TA (µmol kg−1)
DIC (µmol kg−1)
2350
2300
2250
2200
2150
2100
1900
2000
2100
2200
2300

Figure 4